

Hydrogels of Poly(acrylamide-co-acrylic acid): *In-vitro* Study on Release of Gentamicin Sulfate

A. Thakur,* R. K. Wanchoo, and P. Singh

University Institute of Chemical Engineering and Technology
Panjab University, Chandigarh 160 014, India

Original scientific paper

Received: August 30, 2011

Accepted: January 3, 2012

Poly(acrylamide-co-acrylic acid) hydrogels, poly(AAm-co-AAc), were synthesized by free radical polymerization in solution using N,N'-methylenebisacrylamide (MBAAm) as the crosslinker. The structural parameters and the swelling behavior of the synthesized hydrogels were investigated for varying nominal crosslinking ratio and composition of the hydrogels. The use of hydrogels for drug release was investigated with gentamicin sulfate (GS) as the model drug. The drug release from hydrogels was investigated as a function of hydrogel composition, nominal crosslinking ratio (X) and drug loading. The observed drug release data was fitted to a power law model and the power law exponent (n) suggested that the drug release mechanism from these hydrogels was sensitive to hydrogel composition and was swelling-controlled for low concentrations of AAc and showed Fickian diffusion for high concentrations of AAc in the hydrogels. Thermogravimetric analysis (TGA) and differential scanning calorimetry (DSC) studies were performed on control hydrogel samples and drug loaded hydrogels to understand the chemical interactions between the drug and the polymer. Specific drug interactions were observed in these hydrogels.

Key words:

Acrylamide, acrylic acid, hydrogels, crosslinking, swelling, poly(acrylamide-co-acrylic acid), gentamicin sulfate

Introduction

Hydrogels are three-dimensional crosslinked polymeric structures which are able to absorb and retain a large amount of water while remaining insoluble in aqueous solutions.¹ A wide range of hydrophilic polymers have been examined as potential candidates for use in pharmaceutical and medical field as implants, controlled drug release devices, enzyme immobilization, as artificial skin, contact lenses and other uses,^{2–5} due to characteristic properties such as biocompatibility, swellability in water, high water content and rubbery nature which is similar to natural tissue.^{1–6} Special attention has been directed in recent years towards hydrogels that display a change in their dynamic and equilibrium swelling properties in response to external stimuli. It is known that the swelling behavior of any polymer network depends upon the nature of the polymer, the polymer-solvent compatibility and the degree of crosslinking. Depending upon the polymer, these hydrogels can undergo significant volume changes in response to slight changes in environment which can involve pH, temperature, ionic strength, buffer composition etc.^{7–10} In case of anionic polymeric networks, ionization takes place as

the pH of the external medium rises above the pKa of the ionizable moiety.¹¹ The polymeric network becomes more hydrophilic as the degree of ionization increases and the drug release is accomplished as the polymer swells. Polyacrylamide hydrogels, poly(AAm), can absorb relatively high amounts of water; however their swelling capacity is not very sensitive to pH or electrolytes.¹²

Hydrogels of copolymers of acrylic acid (AAc) with acrylamide (AAm) and its derivatives, have been reported with adjustable swelling kinetics with applications for insulin release,¹³ to improve osteoblast adhesion¹⁴ and showing special properties such as super-absorbent hydrogels.^{11,15} Recently, the structural parameters and dynamic swelling behavior of poly(AAm-co-AAc) hydrogels have been investigated as a function of AAc concentration in hydrogels and crosslink density at different pH conditions. The results indicate the diffusion mechanism to be non-Fickian.¹⁶ Owing to the existence of hydrophilic $-\text{COOH}$ and $-\text{NH}_2$ groups, the swelling behavior of these hydrogels is highly dependent on the pH of the surrounding medium. The water content of hydrogels at equilibrium swelling condition is one of the basic properties that makes them useful in drug delivery applications, because hydrogels with high water content are generally considered to be more advantageous as they offer

*Corresponding author: e-mail: anupamat@pu.ac.in;
Tel.: +91-0172-2534930; Fax: +91-0172-2779173

increased permeability and biocompatibility. The development of a drug delivery system requires the control of water content within the polymeric structure, hydrogels based on poly(AAm) and poly(AAc) have the capacity to absorb a substantial amount of water which makes them potential candidates for drug delivering systems.

The present work describes the *in-vitro* release studies of gentamicin sulfate as the model drug from poly(AAm-co-AAc) hydrogels as a drug delivery system. The hydrogels were prepared by free radical copolymerization of AAm and AAc with MBAAm as the bifunctional crosslinking agent and ammonium persulfate (APS) and tetraethylene methylenediamine (TEMED) as the redox initiator system.¹⁶ Poly(AAm-co-AAc) hydrogels were prepared by changing the initial mole ratio of AAm to AAc and MBAAm concentration. The use of hydrogels for drug release was investigated with gentamicin sulfate (GS) taken as the model drug. GS, an aminoglycoside antimicrobial agent having a wide spectrum of antimicrobial activity, is still considered a cornerstone in the treatment of severe infections caused by gram-negative aerobic bacteria.¹⁷

Experimental

Materials

AAc procured from CDH (synthesis grade), was purified by distillation under reduced pressure. AAm (CDH, electrophoresis grade) was used as received without further purification. MBAAm, (Merck, electrophoresis grade) was employed as the crosslinker for the synthesis of hydrogels without further purification. APS, the initiator, and TEMED, the accelerator, were used as a redox initiator pair and were supplied by Merck (A.R.). GS was received as a gift from M/S Ind-Swift laboratory, Parwanoo, India. It was used without further purification. Ninhydrin (Sisco Research Lab, A.R.) and pyridine (Merck,

A.R.) were used as received. Potassium dihydrogen phosphate, sodium hydroxide and all other reagents were of analytical grade and double-distilled deionised water was used throughout.

Hydrogel synthesis

The hydrogels were synthesized using a procedure based on the simultaneous radical polymerization and crosslinking of AAm and AAc.¹⁶ The polymerization mixture was composed of monomers (AAm and AAc), crosslinker (MBAAm), water as solvent and redox initiator (APS and TEMED). Table 1 lists the sample designation and composition of the various hydrogels used in this study. The hydrogels obtained were soft and elastic and uniformly cut into samples of short cylindrical shape with a sharp blade. The samples were first dried at room temperature and finally under vacuum at 40 °C to constant mass, and stored in desiccators containing calcium chloride anhydrous (a desiccant agent, CDH) for further use. The crosslinking ratio (\bar{X}), (defined as moles of crosslinking agent/moles of polymer repeat unit), used in the present study are given in Table 2.

Table 1 – Feed composition and sample designation in the preparation of poly(AAm-co-AAc) hydrogels with MBAAm = 0.2, 0.4, 0.6, 0.8 and 1.0 g/20 g monomer

Sample Code No.	Mass of AAm/g	Mass of AAc/g	AAm/AAc (mole ratio)
A	20.0000	0.0000	100/0
C	17.9747	2.0253	90/10
D	15.9550	4.0450	80/20
E	13.9412	6.0588	70/30
F	11.9328	8.0672	60/40
G	9.9301	10.0700	50/50

Table 2 – Drug diffusion coefficients calculated with early-time approximation for poly(AAm-co-AAc) hydrogels (eq. 4)

Sample	$D \cdot 10^6 \text{ cm}^2 \text{ s}^{-1}$ ($X = 0.0046 \text{ mol mol}^{-1}$)	$D \cdot 10^6 \text{ cm}^2 \text{ s}^{-1}$ ($X = 0.0091 \text{ mol mol}^{-1}$)	$D \cdot 10^6 \text{ cm}^2 \text{ s}^{-1}$ ($X = 0.0137 \text{ mol mol}^{-1}$)	$D \cdot 10^6 \text{ cm}^2 \text{ s}^{-1}$ ($X = 0.0182 \text{ mol mol}^{-1}$)	$D \cdot 10^6 \text{ cm}^2 \text{ s}^{-1}$ ($X = 0.0226 \text{ mol mol}^{-1}$)
A	7.12	6.66	5.05	4.32	3.35
C	6.25	5.2	4.61	3.66	3.27
D	4.25	4.05	3.78	3.18	2.42
E	2.90	2.08	1.19	1.04	0.86
F	2.59	3.25	1.31	1.19	0.95
G	1.58	1.95	–	–	–

Gentamicin sulfate loading in hydrogels

Drug loading was carried out by addition of the drug during the synthesis of the hydrogels. The drug loadings (% mg of drug/g polymer) studied in the present work are 20 %, 30 %, 40 % and 45 %. Briefly, the drug was dissolved in the AAm-AAc-MBAAm monomer solution with continuous stirring under nitrogen atmosphere and then crosslinked by the addition of APS and TEMED under the reaction conditions already discussed in the previous section. The resulting hydrogels were cut uniformly into cylindrical shape samples, dried first at room temperature and finally under vacuum at 40 °C to constant mass, and stored in desiccators containing anhydrous calcium chloride (a desiccant agent, CDH) for further use.

Drug release experiments

Dry hydrogel samples loaded with GS were placed in 20 mL buffer solution of pH 7.4 in glass vials at 37 °C. To follow the release of drug from hydrogel, the hydrogel samples were removed from the vials and immersed in fresh 20 mL of buffer (pre-equilibrated at 37 °C) for continued release at predetermined time intervals. The amount of drug released at each time point was determined spectrophotometrically at 400 nm using a Shimadzu UV-VIS 2450 spectrophotometer. The amount at each time point was added to the amount at all previous points to obtain the cumulative release amount. The distribution of the drug molecules in the hydrogel was assumed to be homogeneous. Control hydrogel samples (samples without gentamicin) immersed in the buffer solution were treated as the blank samples during the assay of gentamicin.

The buffer solution of pH 7.4 was prepared¹⁸ by mixing 50 mL aliquot of a 0.2 mol L⁻¹ monobasic potassium phosphate solution and 39.1 mL of a 0.2 mol L⁻¹ sodium hydroxide solution and diluted to 200 mL with water to form pH 7.4.

Spectrophotometric method of drug estimation

Use of chromatographic, radioimmunoassay and spectrophotometric methods for assaying aminoglycosides have been reported in the literature.¹⁹ Since gentamicin poorly absorbs ultraviolet and visible light, indirect spectrophotometric method for assaying GS is used. The quantitative analysis of gentamicin was done using 10 g L⁻¹ ninhydrin aqueous solution as a derivatizing agent.²⁰ The method is based on the ninhydrin reaction with primary and secondary amines present in the gentamicin producing a purple colour. Gentamicin samples of varying concentrations were prepared in buffer solution of pH 7.4. Aliquot sample of gentamicin solution was mixed with freshly prepared 10 g L⁻¹ ninhydrin aqueous solution and pyridine

was added to it. The mixture was heated in a water bath (Julabo, F20-VC/3) at 70 ± 0.1 °C for 15 min, which resulted in the formation of purple colouring. The tubes were then cooled in an ice-water bath. The UV-visible spectra over the wavelength range of 300–700 nm was measured (using the mixture of gentamicin solution, ninhydrin solution and pyridine) at the appropriate concentrations and the buffer solution as the blanks. Fig. 1 shows the spectrophotometric spectrum of gentamicin sample of 400 µg mL⁻¹ prepared in phosphate buffer of pH 7.4. The scan shows three maxima near 315, 400 and 550 nm. It was observed that the absorbance values at 400 nm of ninhydrin-pyridine-gentamicin mixtures that were heated for 15 min at 70 °C remained virtually unchanged for at least 4 h when kept on ice and protected from light and accordingly absorbance at 400 nm was measured. However, the spectrophotometric examination of all the samples was performed within 1 h. The calibration curve was obtained by linear regression of absorbance – concentration data. The absorbance as a function of concentration followed a linear model up to a concentration of 120 µg mL⁻¹, given by eq. (1):

$$y = 0.01001x \quad (1)$$

where y represents the absorbance and x represents the concentration in µg mL⁻¹. The equation fits the calibration data with a regression coefficient (R^2) of 0.99928, standard error of estimate of 0.08424 and residual standard deviation of 0.07059 (eq. 1).

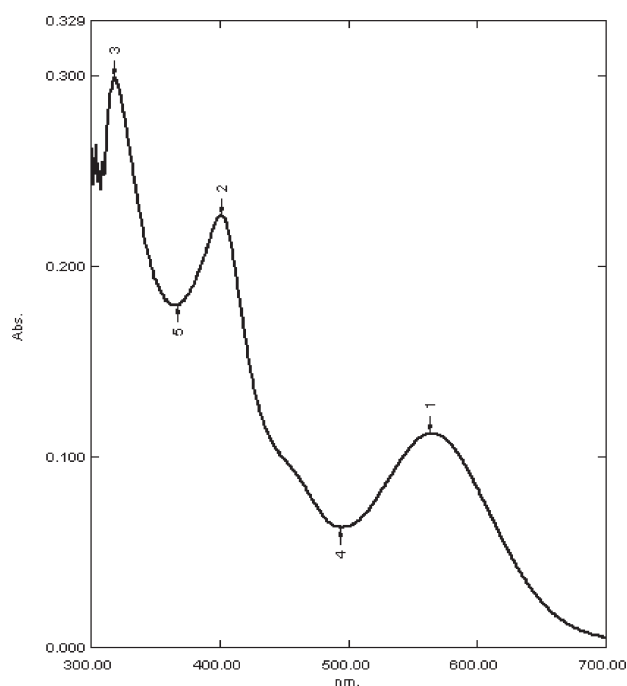


Fig. 1 – Spectrophotometric curve of gentamicin sulfate sample of concentration 400 µg mL⁻¹ in phosphate buffer of pH 7.4

Conditions for gentamicin spectrophotometric method:

2.0 mL gentamicin solution, 2.0 mL ninhydrin reagent, 0.1 mL pyridine, maintained at 70 °C for 15 min, cooled in ice-water bath, dilution to 25 mL, absorbance at 400 nm.

Scanning electron microscopy

SEM analysis of hydrogel samples was carried out using JSM 6100 SEM. Prior to examination, samples were gold-sputter coated to render them electrically conductive.

Thermal analysis

Thermal behavior of hydrogels was studied by thermogravimetric analysis (TGA) and differential scanning calorimetry (DSC). DSC was performed using a Mettler Toledo 821^e (Switzerland) with a TS0801RO Sample Robot. The DSC curves were recorded in the temperature range of 25 to 550 °C at a heating rate of 10 °C min⁻¹, under N₂ atmosphere (50 mL min⁻¹), and evaluated using STARe Software DB V9.00. Thermal gravimetric analysis (TGA) was performed using a TGA/SDTA 851^e Mettler Toledo 821^e with a TS0801RO Sample Robot. TGA thermograms were recorded in the temperature range of 25 to 550 °C at a heating rate of 10 °C min⁻¹, under N₂ atmosphere (40 mL min⁻¹), and evaluated using STARe Software DB V9.00.

Results and discussion

SEM analysis

It is known that the crosslinking ratio and composition of hydrogels affects its microstructure which influences its swelling behavior and hence its drug release characteristics. The structural parameters and swelling characteristics of poly(AAm-co-AAc) hydrogels for some crosslinking ratios have been reported in our previous work.¹⁶ For this, control hydrogel samples were allowed to equilibrate in the medium of study. Hydrogels with higher acrylic acid content presented a more open and porous channel structure due to electrostatic repulsion of the ionic charges of its network in basic buffer. Acrylic acid contains carboxyl groups (–COOH) and the ionization of these groups above its pK_a (4.7) causes the swelling to increase. In the present study, the effect of nominal crosslinking ratio on pore size for hydrogel sample E (70/30) is reported. Fig. 2 presents scanning electron micrographs of hydrogels swollen to equilibrium conditions in buffer solution of pH 7.4 after freeze drying^{21,22} for different crosslinking ratios. Freeze-drying was carried out in vacuum at –50 °C for 24 h using Heto LyoLab 3000 (Denmark) lyophiliser. No crack formation was observed in any of the samples. The cross-sectional views of the hydrogels present an ir-

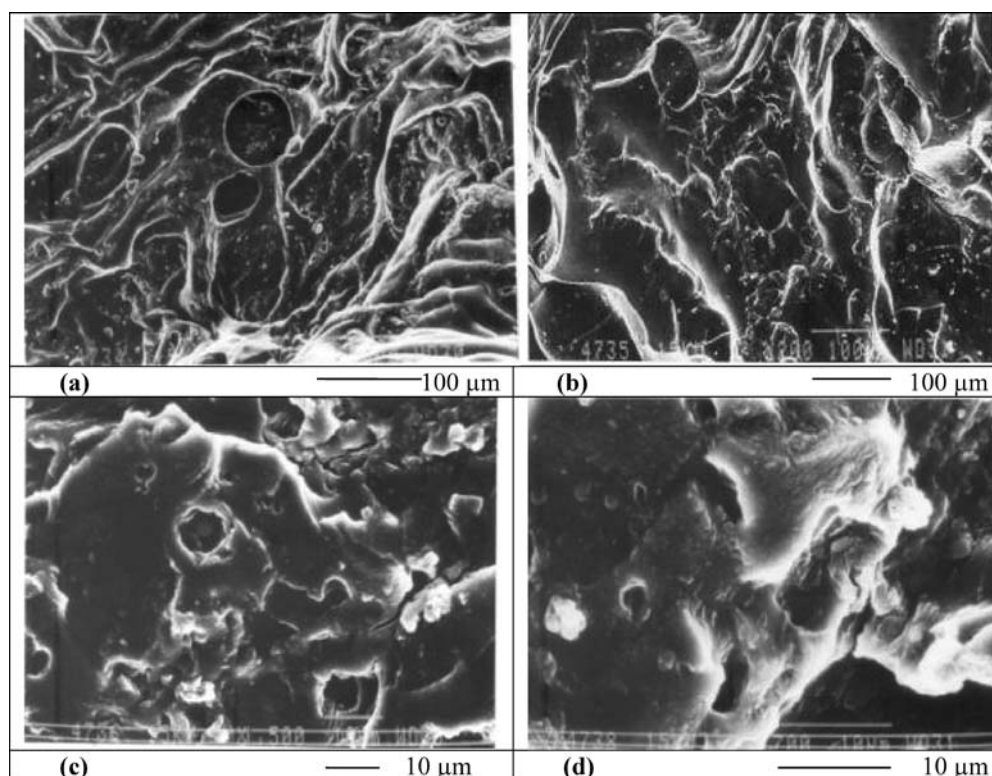


Fig. 2 – Scanning electron micrographs of cross-sections of freeze-dried 70/30 AAm/AAc hydrogels swollen in buffer of pH 7.4 at various nominal crosslinking ratios X , mol mol⁻¹ (a) $X = 0.0046$ (ref. 16) (b) $X = 0.0091$ (ref. 16) (c) $X = 0.0137$ (d) $X = 0.0182$

regular surface pattern with macro/micro pores within the hydrogel. The pore size of hydrogels is found to decrease with increase in MBAAm concentration. Sample E with nominal crosslinking ratio $X = 0.0046$ presents a surface with a pore size varying between 60 – 80 μm . With the incorporation of more crosslinker units in the hydrogel formulation, hydrogels present a different morphology. The hydrogel surface presents pores of size 50 – 60 μm at $X = 0.0091$ and with further increase in MBAAm concentration, the pore size of hydrogel at $X = 0.0137$ is observed to be 7 – 10 μm which

further reduces to about 3 – 5 μm at nominal crosslinking ratio of $X = 0.0182$.

In-vitro drug release

The effect of composition of hydrogels, degree of crosslinking and drug loading was investigated on the release of gentamicin sulfate from hydrogels.

(a) Effect of acrylic acid content

Dried drug-loaded hydrogels were used for the drug release studies. Figs. 3(a-e) show the cumula-

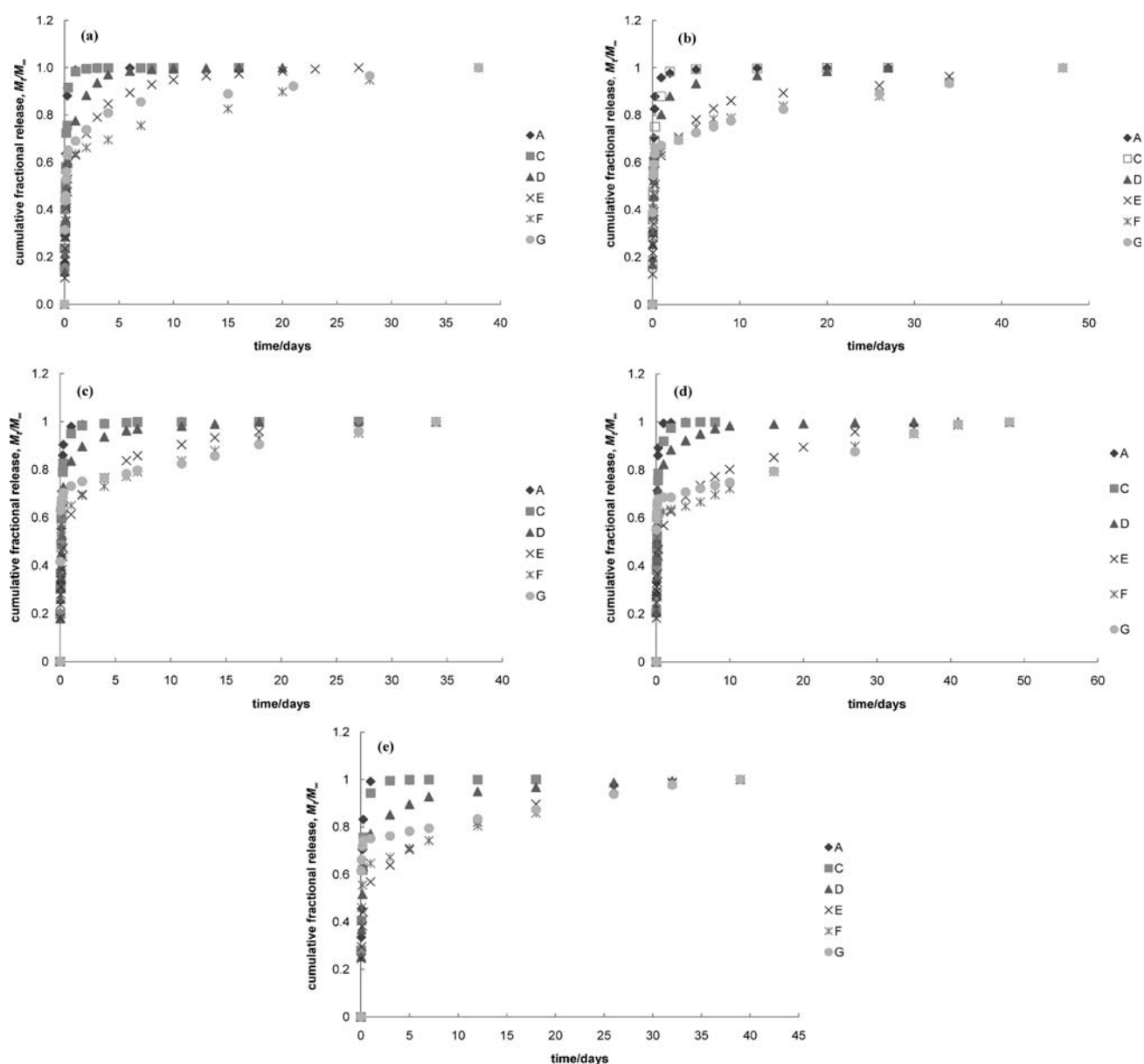


Fig. 3 – (a) Effect of acrylic acid content on release of gentamicin sulfate in buffer of pH 7.4 at 37 °C at nominal crosslinking ratio $X = 0.0046 \text{ mol mol}^{-1}$; (b) Effect of acrylic acid content on release of gentamicin sulfate in buffer of pH 7.4 at 37 °C at nominal crosslinking ratio $X = 0.0091 \text{ mol mol}^{-1}$; (c) Effect of acrylic acid content on release of gentamicin sulfate in buffer of pH 7.4 at 37 °C at nominal crosslinking ratio $X = 0.0137 \text{ mol mol}^{-1}$; (d) Effect of acrylic acid content on release of gentamicin sulfate in buffer of pH 7.4 at 37 °C at nominal crosslinking ratio $X = 0.0182 \text{ mol mol}^{-1}$; (e) Effect of acrylic acid content on release of gentamicin sulfate in buffer of pH 7.4 at 37 °C at nominal crosslinking ratio $X = 0.0226 \text{ mol mol}^{-1}$

tive fractional release of gentamicin sulfate from poly(AAm-co-AAc) samples in phosphate buffer of pH 7.4, at 37 ± 0.1 °C. The data was obtained in triplicate and was reproducible with maximum average error (eq. 2) of 1.5 %.

$$\% \text{ average error} = \frac{\sum_{i=1}^{i=n} |x_i - \bar{x}|}{n} \cdot 100 \quad (2)$$

where x_i represents the experimental value of cumulative fractional drug release (M_t/M_∞) from hydrogel sample at time t , \bar{x} is the mean of three readings, n is the total number of drug release samples taken during drug release studies for a drug-loaded hydrogel sample.

Poly(AAm) hydrogel samples demonstrated a very high burst effect with almost 70 % of the total drug being released within the first 4 hours. This burst effect can be attributed to the dissolution or diffusion of gentamicin sulfate on the surface of the polymer. As the acrylic acid content increased in the hydrogels for a given crosslink ratio, the burst effect was found to decrease substantially. This decrease in burst effect with increasing amount of AAc in hydrogels indicated an acid-base interaction between the amino group of gentamicin and the carboxylic groups present in the polymer chains.²³ The results indicate that with increasing the amount of carboxyl group, the interaction between polymer and drug also increases, which results in a significant decrease in the gentamicin sulfate release.

It was observed during drug release studies that drug-loaded samples showed different swelling and morphological characteristics. The samples did not swell appreciably as compared to blank samples of same composition and crosslinker concentration. This can be attributed to the strong intermolecular complexation due to hydrogen bonding between the carboxylic groups of poly(AAm-co-AAc) and the highly polar cationic drug; further, due to these strong intermolecular forces of attraction, hydrogels did not crack and were observed to be in a swollen state in phosphate buffer over the course of drug release studies for high crosslinker ratios. When the control hydrogel samples were used for swelling studies at similar higher crosslinker ratios, the samples were observed to crack after some time, and hence structural parameters of these hydrogels could not be investigated.

In order to fit the experimental data of drug release, the mathematical solution of Fick's second law of diffusion proposed by Crank²⁴ (eq. (3)) was used. This expression is referred to cylindrically shaped polymer hydrogels, one-dimensional radial release from a cylinder of radius a .

$$\frac{M_t}{M_\infty} = 4 \left(\frac{Dt}{\pi a^2} \right)^{\frac{1}{2}} - \frac{Dt}{a^2} - \frac{1}{3\pi^2} \left(\frac{Dt}{a^2} \right)^{\frac{3}{2}} + \dots \quad (3)$$

Neglecting higher order terms, eq. (3) reduces to:

$$\frac{M_t}{M_\infty} = 4 \left(\frac{Dt}{\pi a^2} \right)^{\frac{1}{2}} \quad (4)$$

where M_t/M_∞ is the cumulative fractional drug release, t is the release time and D is the average diffusion coefficient of the drug in the hydrogel. Eq. (4) is the early-time approximation equation obtained under the initial and boundary conditions tested in this work and is valid for the first 60 % of the data. The early time diffusion coefficients calculated from eq. (4) are reported in Table 2. The diffusion coefficient values lie in the range of $7.12 \cdot 10^{-6} \text{ cm}^2 \text{ s}^{-1}$ to $0.95 \cdot 10^{-6} \text{ cm}^2 \text{ s}^{-1}$ for various nominal crosslinking ratios and compositions of hydrogels. It may be mentioned here that diffusion coefficient of the same order of magnitude has also been reported by Simovic *et al.*²⁵ for GS in phosphate buffer of pH 7.4.

A simple empirical equation based on a power law expression, relating cumulative fractional release of drug to the release time, is one of the most widely used to interpret release data for swelling controlled devices. The equation popularly known as Ritger and Peppas equation^{6,16} is as follows:

$$\frac{M_t}{M_\infty} = kt^n \quad (5)$$

where n denotes the type of transport mechanism for drug diffusion through the polymer and k is a kinetic constant. For cylindrical geometry, the value of diffusional exponent n as 0.45 signifies a Fickian diffusion mechanism, while $n \geq 0.89$ is Case II diffusion mechanism which indicates zero order release behavior, while the value of n in the range $0.45 < n < 0.89$, indicates that diffusion mechanism is anomalous or non-Fickian, where both diffusion and polymer relaxation control the overall rate of solute transport.⁷ To determine whether the diffusion rate was controlled by Fickian type diffusion or swelling of polymer or both, first 60 % of drug release data was fitted to Ritger and Peppas equation (eq. 5) and the effect of composition of hydrogels on the drug mass transport mechanism was analyzed. The values of the drug diffusion exponent n , obtained for gentamicin sulfate release in phosphate buffer for the hydrogels are reported in Table 3.

Table 3 – Drug release index for poly(AAm-co-AAc) hydrogels (eq. 5)

Sample	$X = 0.0046$		$X = 0.0091$		$X = 0.0137$		$X = 0.0182$		$X = 0.0226$	
	mol mol ⁻¹		mol mol ⁻¹		mol mol ⁻¹		mol mol ⁻¹		mol mol ⁻¹	
	n	k	n	k	n	k	n	k	n	k
A	0.7582	0.0006	0.7262	0.0008	0.6444	0.0016	0.5892	0.0027	0.5400	0.0039
C	0.6570	0.0011	0.6373	0.0015	0.6028	0.0021	0.5441	0.0034	0.5190	0.0041
D	0.5957	0.0016	0.5444	0.0029	0.5140	0.0038	0.4780	0.0059	0.4428	0.0071
E	0.4856	0.0037	0.4372	0.0059	0.3536	0.0132	0.3395	0.0147	0.3101	0.0196
F	0.3587	0.0152	0.2995	0.0315	0.2420	0.0588	0.2163	0.0692	0.2043	0.0771
G	0.2570	0.0480	0.1769	0.1114	–	–	–	–	–	–

It was observed that an increase in acrylic acid content of hydrogels yields a change in the drug release mechanism from anomalous diffusion to Fickian diffusion. The value of n was found to decrease with increase in acrylic acid content of hydrogels indicating that the relative contribution of relaxation process of polymer reduces and becomes diffusion controlled. This indicates that the hydrogels serve as a diffusion barrier and the drug releases mainly by diffusion mechanism supported by swelling behavior.

(b) Effect of nominal crosslinking ratio and drug loading on drug release

The influence of nominal crosslinking ratio, X , on the release of gentamicin sulfate from hydrogels was investigated. Fig. 3(a-e) shows the cumulative fractional release from poly(AAm-co-AAc) hydrogels at different crosslinking ratios and Fig. 4 shows the cumulative fractional release from sample E with a drug loading of 30 % at different crosslinking ratios. The diffusion exponent n evaluated from eq. (5) for drug release from hydrogel samples A and C (Table 3) was found to be more than 0.45 for all crosslinking ratios, thereby indicating that non-Fickian diffusion plays an important role in drug release from these hydrogels. However, for hydrogels other than labeled as A and C, diffusion exponent n depended on crosslinker concentration to be termed as either Fickian or non-Fickian diffusion. These results indicate that with an increase in crosslink ratio, there is a decrease in pore size of the hydrogel structure; it becomes more compact resulting in a decrease in the amount of drug released. As a result, the drug release rate from hydrogels with a high crosslinking ratio decreases because of the increase in crosslinking density.

Fig. 5 shows the effect of drug loading on the release pattern as a function of time, in poly(AAm-co-AAc) hydrogels, (sample E), with a nominal crosslinking ratio $X = 0.0091$ (mol mol⁻¹).

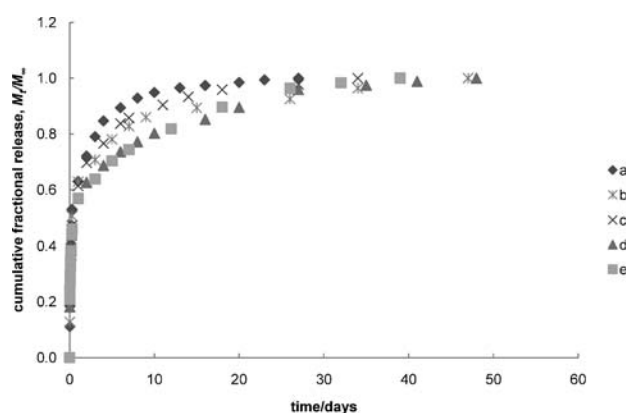


Fig. 4 – Effect of nominal crosslinking ratio X (mol mol⁻¹) on gentamicin release from sample E with 30 % drug loading in buffer of pH 7.4, 37 °C (a) $X = 0.0046$ (b) $X = 0.0091$ (c) $X = 0.0137$ (d) $X = 0.0182$ (e) $X = 0.0226$

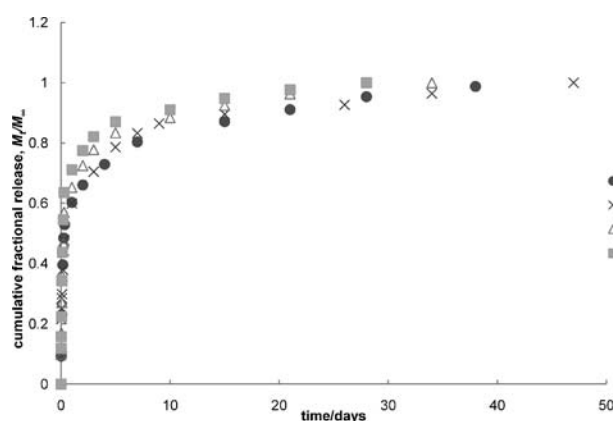


Fig. 5 – Effect of drug loading (%) on its rate of release from sample E at $X=0.0091$ mol mol⁻¹ in buffer of pH 7.4, 37 °C (a) 20 % (b) 30 % (c) 40 % (d) 45 %

Hydrogel samples with high drug loadings show large initial bursts due to more drug clusters connected to the hydrogel surface. At any given time, the drug release increased with the increase in percent loading of the gentamicin sulfate in hydrogels in phosphate buffer (pH 7.4) at 37 ± 0.1 °C. The cu-

mulative fractional release plots suggest that at lower concentration of drug, most of the drug molecules remain bounded with carboxylic acid of the poly(AAc) chain of the hydrogels, whereas, at higher concentration of drug in hydrogel samples, the percentage of unbounded drug molecules increases in the polymer networks. Gentamicin sulfate is freely soluble in phosphate buffer (pH 7.4). As a result, the rate of depletion of drug in polymer at higher concentration is faster than at lower concentration of drug. In this process, the hydrogel becomes more porous at high drug concentration, and this increases the diffusion constant of drug in polymer network.^{23,26} The early-time diffusion coefficients (using eq. (4)) for poly(AAm-co-AAc) hydrogels, (sample E), with a nominal crosslinking ratio $X = 0.0091$ (mol mol⁻¹) at various drug loading are tabulated in Table 4.

Table 4 – Drug diffusion coefficients calculated with early-time approximation for poly(AAm-co-AAc) hydrogels, sample E, at $X = 0.0091$ mol mol⁻¹, for various drug loading (%) (a) 20 %, (b) 30 % (c) 40 % (d) 45 % using eq. 4

Sample	$D \cdot 10^6$ cm ² s ⁻¹ (a)	$D \cdot 10^6$ cm ² s ⁻¹ (b)	$D \cdot 10^6$ cm ² s ⁻¹ (c)	$D \cdot 10^6$ cm ² s ⁻¹ (d)
E	1.25	2.08	2.27	3.29

Thermal analysis

Thermal behavior of the control hydrogels and drug-loaded hydrogels was studied by TGA and DSC to determine the existence of possible interaction between the polymer and drug. Fig. 6(a) shows the TGA scan of dried sample of poly(AAm) hydrogel with a crosslinking ratio of 0.0091. It is observed that the decomposition of poly(AAm) hydrogel starts at 225 °C and is complete at nearly 460 °C. The total degradation of hydrogel is observed to take place in three stages. In the first stage a mass loss of about 12 % occurs, and the second stage beginning at 225 °C, occurs with a mass loss of about 14 % at 350 °C. The last stage up to 460 °C is characterized by a mass loss of 46 %. The mass loss occurring in the first stage of temperature is attributed to the evaporation of water molecules from the hydrogel. DSC curve of poly(AAm) hydrogel is shown in Fig. 6(b). It is observed that an endothermic peak is obtained at nearly 72.41 °C. Another transition is observed in the temperature range of 180 – 200 °C as a small kink. A similar observation has been reported by Iwahara,²⁷ and this has been analyzed as the glass transition temperature T_g (transition from a glassy state to a visco-

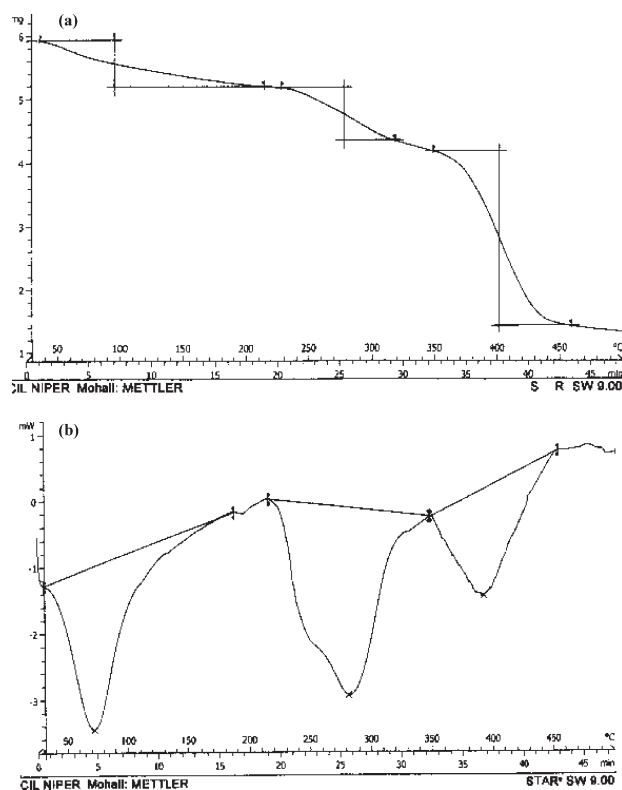


Fig. 6 – (a) TGA curve of poly(AAm) hydrogel at $X = 0.0091$ mol mol⁻¹; (b) DSC curve of poly(AAm) hydrogel at $X = 0.0091$ mol mol⁻¹

elastic state) which takes place at a temperature of about 190.45 °C. The peak at 72.41 °C can be ascribed to the loss of water, which could not be removed completely from the hydrogels on drying.

The TGA curve of the dried sample of poly(AAm-co-AAc) hydrogel (sample E, $X = 0.0091$ mol mol⁻¹) in Fig. 7(a) shows three degradation steps. A mass loss of about 10 % occurs in the first stage. The second stage ranging from 210 – 258 °C occurs with a mass loss of about 8 %. The third stage represents the total degradation of the hydrogel, with a maximum at 370 °C and a mass loss of about 62 %. It is observed that beyond 258 °C, the hydrogel continues to absorb heat and decomposes finally at 500 °C. Fig. 7(b) shows the DSC scan of the same hydrogel. The glass transition is observed as a small endotherm at approximately 178.35 °C. The other endothermic peak occurring at 75.59 °C is due to the evaporation of water from the hydrogel with an enthalpy change of 163 J g⁻¹.

The thermal behavior of dried sample of poly(AAc) hydrogel was also studied and is shown in Fig. 8(a, b) as a TGA and DSC scan. The thermal degradation of polymer essentially takes place in two stages. A mass loss of about 1.8 % up to 120 °C occurs before the start of first stage of thermal degradation, which is due to the loss of water molecules from the hydrogel. The first stage began

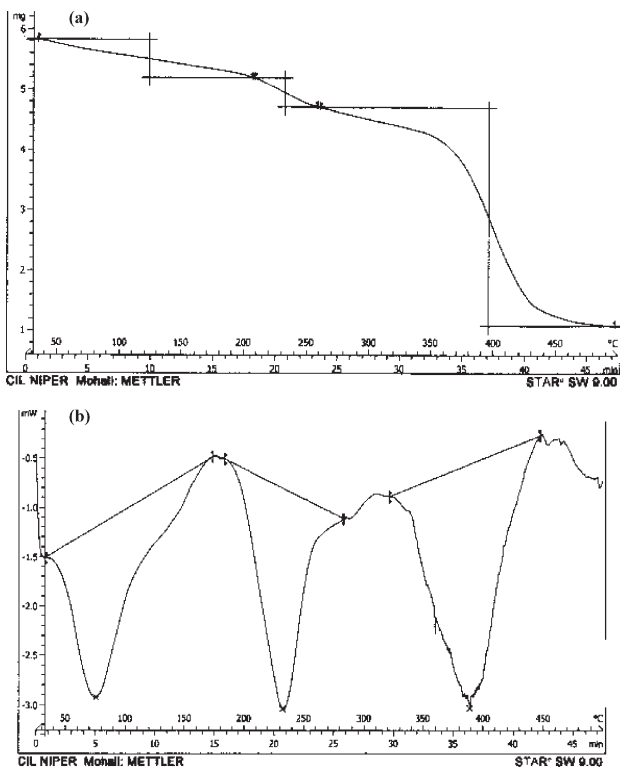


Fig. 7 – (a) TGA curve of poly(AAm-co-AAc) hydrogel, sample E, at $X = 0.0091 \text{ mol mol}^{-1}$; (b) DSC curve of poly(AAm-co-AAc) hydrogel, sample E, at $X = 0.0091 \text{ mol mol}^{-1}$

at approximately 120 °C and reached a maximum at 278 °C with a mass loss of about 29 %. The degradation of the polymer is more rapid in the second stage, which starts at 308 °C with a mass loss of about 60 % up to 550 °C. From the DSC scan (Fig. 8(b)), it is obvious that a transition occurs over a relatively narrow temperature range, 65 – 70 °C. The second transition is visible at approximately 105 °C which is very close to the T_g value of 106 °C reported for poly(AAc) in literature.²⁸ From the DSC profiles of the above hydrogels (Fig. 6(b), 7(b), 8(b)), it is also observed that water has a higher evaporation temperature in the poly(AAm-co-AAc) hydrogel copolymer (75.59 °C) than in poly(AAc) hydrogel (65 – 70 °C) and poly(AAm) hydrogel (72.41 °C) suggesting that the interaction between water molecules and copolymer network are more numerous than in homopolymer hydrogels.

Both poly(AAm) and poly(AAc) hydrogel are glassy polymers as their glass transition temperatures are well above the room temperature. The compatibility between two glassy polymers in solid state can be assessed by, whether the glass transition temperature T_g obeys Fox equation. T_g of poly(AAm) and poly(AAc) was determined to be 190.45 °C and 105 °C respectively (Fig. 6(b), 8(b)). The T_g of copolymer was calculated according to the Fox equation:²⁹

$$\frac{1}{T_g} = \frac{w_1}{T_{g1}} + \frac{w_2}{T_{g2}} \quad (6)$$

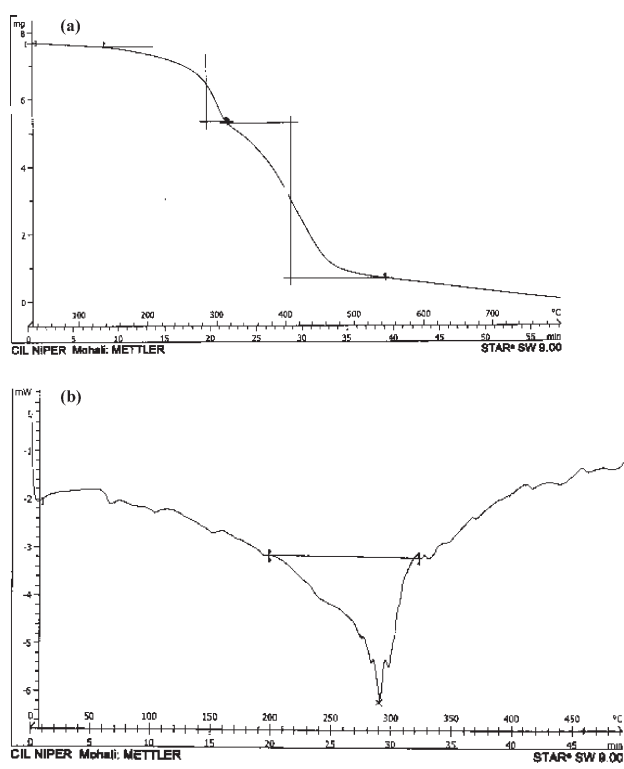


Fig. 8 – (a) TGA curve of poly(AAc) hydrogel at $X = 0.0091 \text{ mol mol}^{-1}$; (b) DSC curve of poly(AAc) hydrogel at $X = 0.0091 \text{ mol mol}^{-1}$

where T_{g1} and T_{g2} are the glass transition temperatures of poly(AAm) and poly(AAc), w_1 and w_2 are the mass fractions of poly(AAm) and poly(AAc) respectively. The DSC scan of hydrogel sample E showed a single T_g transition, approximately at 178.35 °C, which is between that of poly(AAm) and that of poly(AAc). Using the Fox equation, the glass transition temperature of copolymer turns out to be 153.1 °C. The presence of additives like MBAAM, method of synthesis, molecular mass and the possible interaction of poly(AAm) with poly(AAc) are some factors which may be responsible for the observed variance of experimentally determined T_g values of poly(AAm-co-AAc) hydrogel.

Figs. 9(a, b) show the DSC and TGA curves of the pure drug gentamicin sulfate (GS). GS is a complex mixture of the sulfates of gentamicin C_1 (melting point (m. pt.) 94 – 100 °C), gentamicin C_{1a} and gentamicin C_2 (m. pt. 107 – 124 °C). Some commercial samples may contain significant quantities of the minor components gentamicin C_{2a} and gentamicin C_{2B} . The melting point (m. pt.) of the C complex sulfate is given as 218 – 237 °C.^{30,31} In the thermogram, Fig. 9(a), a broad endothermic peak at 103.83 °C and peaks at 244.77, 252.38 and

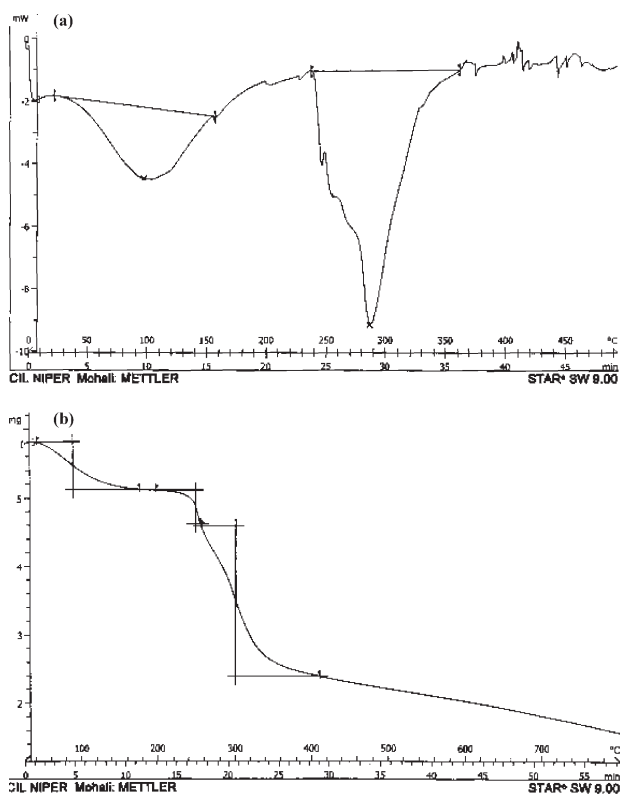


Fig. 9 – (a) DSC curve of the pure drug gentamicin sulfate (GS); (b) TGA curve of the pure drug gentamicin sulfate (GS)

287.43 °C were observed. These peaks seem to correspond to the m. pt. of the components of GS complex. The thermal degradation of the pure drug took place in three stages as shown in Fig. 9(b). In the first stage, a mass loss of 11.84 % occurred followed by a rapid mass loss in the second and third stages. A mass loss of 8.65 % occurred in the second stage with a peak temperature at 225 °C. The third stage is characterized by total degradation with a mass loss of 37.89 % up to 405 °C.

Drug-polymer interaction

To examine the interaction of gentamicin sulfate (GS) with the polymer, DSC thermogram of the pure GS was compared with the thermogram of poly(AAm) and poly(AAm-co-AAc) polymer hydrogel loaded with GS. Fig. 10(a) shows the DSC curve of poly(AAm-co-AAc), (sample E, $X = 0.0091 \text{ mol mol}^{-1}$), loaded with GS. It is observed that the characteristic sharp peak at 286.6 °C which corresponds to the m. pt. of one of the components of the gentamicin sulfate complex is missing in the thermogram, whereas, a sharp endothermic peak at 324.53 °C is observed suggesting the formation of an ion pair between the carboxylic acid group of the polymer and the amino group of the GS. As reported in literature, an interaction is known to occur between drug and polymer if ap-

pearance of new peaks or disappearance of peaks is observed.³² Moreover, the sharp peaks observed in the DSC curve of pure drug which occur at 244.77, 252.38 and 287.43 °C corresponding to the m. pt. of other components of C complex sulfate of gentamicin are not observed as sharp peaks. Instead, a broad endothermic peak in the temperature range of 230 – 250 °C is observed suggesting interaction between the polymer and the drug. Another peak observed in DSC curve at 390.24 °C seems to be due to degradation of polymer/drug present in the polymer. A broad endothermic peak observed at 72.90 °C is probably due to the loss of water molecules from the polymer-drug sample. The TGA curve (Fig. 10(b)) of the polymer-drug sample shows three stages of degradation. A mass loss of 11.3 % occurs in the first stage up to about 205 °C. In the second stage a mass loss of about 22 % occurs, and the third stage starting at about 335 °C shows the final degradation of the polymer with a mass loss of 37.51 %, and is complete at 500 °C.

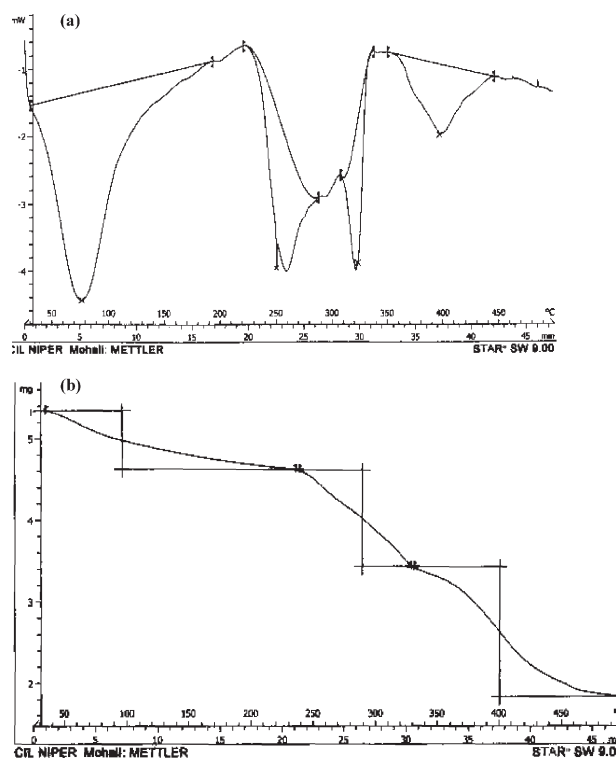


Fig. 10– (a) DSC curve of drug-loaded poly(AAm-co-AAc) hydrogel, sample E, at $X = 0.0091 \text{ mol mol}^{-1}$; (b) TGA curve of drug-loaded poly(AAm-co-AAc) hydrogel, sample E, at $X = 0.0091 \text{ mol mol}^{-1}$

DSC curve of poly(AAm) polymer hydrogel loaded with GS drug is shown in Fig. 11(a). The peaks occurring at 244.77 °C and 252.38 °C in the DSC scan of pure drug (Fig. 9(a)) are found to shift to 250.13 °C and 260.13 °C in drug-loaded poly(AAm) polymer hydrogel. The slight shift ob-

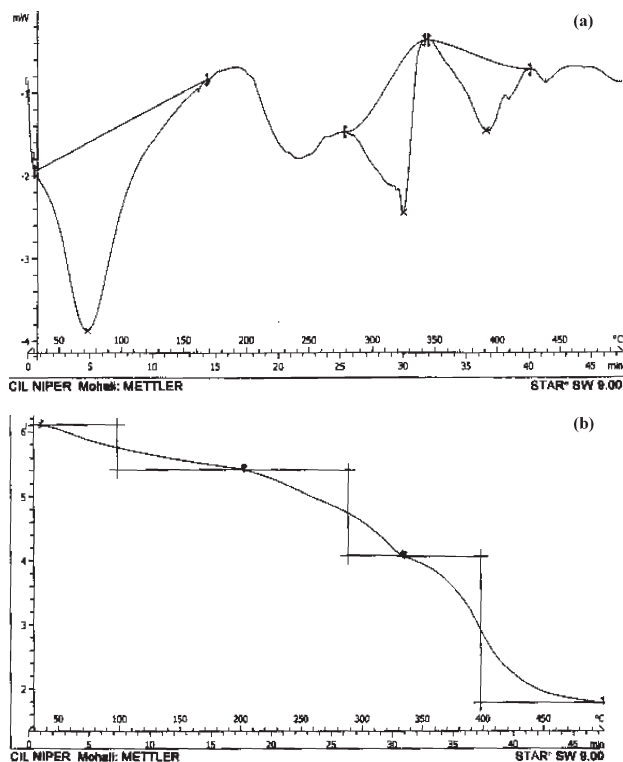


Fig. 11 – (a) DSC curve of drug-loaded poly(AAm) hydrogel at $X = 0.0091 \text{ mol mol}^{-1}$; (b) TGA curve of drug-loaded poly(AAm) hydrogel at $X = 0.0091 \text{ mol mol}^{-1}$

served in the drug peaks in poly(AAm)-drug sample may be due to mixing with the polymer³¹ and the possible existence of poly(AAm) in a slightly hydrolysed state resulting in a weak interaction between the drug and polymer. However, an endothermic peak observed at 322.78 °C may be due to degradation of polymer/drug present in the polymer. From the above results, it may safely be concluded that the changes observed in the thermal features of poly(AAm-co-AAc)-drug sample and the appearance of new peaks clearly support the interaction of drug with the poly(AAm-co-AAc) hydrogel, and since no new peaks are observed in poly(AAm)-drug sample, it also confirms the absence of interaction between the drug and poly(AAm) hydrogel. This explains the sudden release of drug from the poly(AAm) hydrogel whereas a comparatively slow rate of drug release was observed in the case of poly(AAm-co-AAc) hydrogel samples, with dependence on hydrogel composition crosslinker ratio.

Conclusions

In this study poly(AAm-co-AAc) hydrogels were synthesized by radical polymerization in solution at different crosslinking ratios and loaded with gentamicin sulfate as the model drug. The results indicated that release of gentamicin sulphate from

hydrogels is dependent on the composition of the hydrogels, crosslinking ratio and concentration of drug in the polymer. The release pattern followed a two-step pattern, with an initial burst followed by a slow and continuous release. The diffusion exponent signifying Fickian diffusion or anomalous diffusion for the drug release curve in phosphate buffer depends upon the degree of crosslinking and hydrogel composition, and the conditions could be optimized for the release of drug from these pH sensitive hydrogels to be used as drug delivery systems. Thermal analysis of control hydrogels and drug-loaded hydrogels indicated the existence of strong interactions between the polymer and the drug.

ACKNOWLEDGEMENTS

This work was supported by the All India Council for Technical Education (AICTE), Govt. of India, through grant no. 8023/RID/RPS-50/2004-05.

List of symbols

- a – radius of cylindrical hydrogel sample, cm
- D – diffusion coefficient, $\text{cm}^2 \text{s}^{-1}$
- k – kinetic constant
- n – diffusion exponent
- M_t/M_∞ – cumulative fractional drug release from hydrogel sample at time t
- t – time, s
- T_g – glass transition temperature, °C
- X – nominal crosslinking ratio, mol mol^{-1}
- w – mass fraction, %

References

1. Hoffman, A. S., Adv. Drug Del. Rev. **54** (2002) 3.
2. Netti, P. A., Shelton, J. C., Revell, P. A., Pirie, C., Smith, S., Ambrosio, L., Nicolais, L., Bonfield, W., Biomaterials **14** (1993) 1098.
3. Young, C. D., Wu, J. R., Tsou, T. L., J. Membr. Sci. **146** (1998) 83.
4. Brinkman, E., van der Does, L., Bantjes, A., Biomaterials **12** (1991) 63.
5. Abusafieh, A., Siegler, S., Kalidindi, S. R., J. Biomed. Res. **38** (1997) 314.
6. Peppas, N. A., Bures, P., Leobandung, W., Ichikawa, H., Eur. J. Pharm. Biopharm. **50** (2000) 27.
7. Alarcón, Carolina de las H., Sivanand, P., Cameron, A., Chem. Soc. Rev. **34** (2003) 276.
8. Brondsted, H., Kopecek, J., Biomaterials **12** (1991) 584.
9. Gupta, P., Vermani, K., Garg, S., Drug Discov. Today **7** (2002) 569.
10. Akala, E. O., Kopeckova, P., Kopecek, J., Biomaterials **19** (1998) 1037.
11. Dhara, D., Nisha, C. K., Chatterji, P. R., JMSF Pure Appl. Chem. **A36** (1999) 197.

12. Wahlig, H., Dingeldien, E., Bergmann, R., Reuss, K., *J. of Bone and Joint Surgery* **60B**(2) (1978) 270.
13. Vernon, B., Kim, S. W., Bae, Y. H., *J. Biomater. Sci., Polym. Ed.* **10** (1999) 183.
14. Bearinger, J. P., Castner, D. G., Healy, K. E., *J. Biomater. Sci., Polym. Ed.* **9** (1998) 629.
15. Aoki, T., Kawashima, M., Katono, H., Sanui, K., Ogata, N., Okano, T., Sakurai, Y., *Macromol.* **27** (1994) 947.
16. Thakur, A., Wanchoo, R. K., Singh, P., *Int. J. Chem. Biochem. Eng. Q.* **25**(2) (2011) 181.
17. Isoherranen, N., Soback, S., *Clin. Chem.* **46** (2000) 837.
18. The United States Pharmacopeia, Vol XXII, 21st Revision, Mack Publishers, Easton, 1985.
19. Sampath, S. S., Robinson, D. H., *J. Pharm. Sci.* **79** (1990) 428.
20. *Clark's Isolation and Identification of Drugs*, 2nd ed., The Pharmaceutical Press, London, 1989.
21. Caliceti, P., Salmaso, S., Lante, A., Yoshida, M., Katakai, R., Martellini, F., Mei, L. H. I., Caranza, M., *J. Control. Rel.* **75** (2001) 173.
22. Risbud, M. V., Bhonde, R. R., *Drug Del.* **7** (2000) 69.
23. Brazed, C. S., Peppas, N. A., *Eur. J. Pharm. Biopharm.* **49** (2000) 47.
24. Crank, J., *The mathematics of diffusion*, Clarendon press, Oxford, 1975.
25. Simovic, L., Skundric, P., Lijakovic, I. P., Ristic, K., Medovic, A., Tasic, G., *J. Appl. Polym. Sci.* **117** (2010) 1424.
26. Siepmann, J., Gopferich, A., *Adv. Drug Del. Rev.* **48** (2001) 229.
27. Iwahara, K., Hirata, M., Honda, Y., Watanabe, T., Kuwahara, M., *Biotechnol. Lett.* **22** (2000) 1355.
28. Brandrup, J., Immergut E. H., *Polymer handbook*, 3rd ed., New York, Wiley –Interscience, VII-215, 1989.
29. Billmeyer, F. W., Jr., *Textbook of polymer science*, 3rd ed., Wiley –Interscience, 1984.
30. *The Merck Index*, 13th ed., p-780, 2001.
31. *Martindale: The Complete Drug Reference*, 32nd ed., Pharmaceutical Press, London, ed. K. Parfitt, 1999, p-212.
32. Milallos, R. G., Alexander, K., Riga, A., *J. Therm. Anal. Calorim.* **93** (2008) 289.